

1
2
3

The direct read-out of organic and inorganic scintillators with the Multi Pixel Photon Counter

4 Nicola D'Ascenzo^{a,b,*}, E. Garutti^b, M. Goettlich^b,
5 H.C. Schultz-Coulon^c, A. Tadday^c

6 ^a*University of Hamburg, Edmund-Siemers-Allee 1, D-20146, Hamburg, Germany*

7 ^b*DESY, Notkestr. 85, D-22607 Hamburg, Germany*

8 ^c*University of Heidelberg, Im Neuenheimer Feld 227, D-69120 Heidelberg,*
9 *Germany*

10 **Abstract**

11 The Micro Pixel Photon Counter (MPPC) is a new silicon-based photo-detector
12 developed by Hamamatsu. Its key-features are the small active area, the easy biasing
13 and read-out circuit, the high gain and the optimisation of the sensitivity in the blue
14 spectral region. Hence the MPPC seems to be the ideal candidate for the read-out
15 of radiation detection devices which are based on a large number of fast scintillator
16 arrays.

17 In this paper we study the direct read-out of organic and inorganic (LSO and
18 LSF crystals) scintillators via MPPC, with the aim to investigate their technolog-
19 ical potential for the design of highly granular positron emission tomographs and
20 calorimeters.

21 *Key words:* Photo-detectors, Silicon PhotoMultiplier, MPPC, calorimetry, PET

22 *PACS:* 29.40.Vj, 29.40.Mc, 29.40.Wk, 29.40.Ej, 87.57.uk

23 **Introduction**

24 Silicon pixel photo-detectors operated in Geiger mode [1–3] are a new sort
25 of silicon-based photo-detectors. Their active area ranges between $1 \times 1 \text{ mm}^2$
26 and $5 \times 5 \text{ mm}^2$ and they are very easy to operate. They reach, in fact, a gain

* Corresponding author

Email address: nicola.dascenzo@desy.de (Nicola D'Ascenzo).

27 up to 10^6 with a relative low voltage supply typically ranging between 30 V
28 and 70 V. The resulting current signal is sizable even for a single detected
29 photon and has a rise time of less than 100 ps. It can be extracted with a
30 simple electronic circuit, usually just with a large bandwidth voltage amplifier.
31 In addition, this photo-detector is insensitive to strong magnetic fields. The
32 first devices of this family, so called Silicon PhotoMultipliers (SiPM), have a
33 sensitivity mainly peaked in the green spectral region. The Micro Pixel Photon
34 Counter (MPPC) tested in this paper have been developed by Hamamatsu [4]
35 and inherits all the properties of the SiPM. Moreover, for the first time, they
36 provide very good sensitivity in the blue spectral region.

37 There is a big interplay between the improvements in the Silicon Photomultiplier
38 technology and the research and development of many scintillator based
39 detectors, ranging from particle physics to space and medical applications.
40 The aim of this paper is to investigate if some of the benchmarks properties
41 of the photodetectors for highly granular calorimetry and positron emission
42 tomography are satisfied by the MPPC.

43 Calorimeters are devices dedicated to the measurement of the energy of par-
44 ticles. This measurement is a experimental challenge at high energy colliders,
45 due to the dense multi-jet environment. A lateral granularity and a longitu-
46 dinal segmentation of few centimeters would allow the reconstruction of the
47 topology of the showers induced by each single particle within a jet. The dif-
48 ferent treatment of electromagnetic, hadronic and neutral components would
49 improve the energy resolution. The instrumentation of such detector is a dif-
50 ficult technological task. Millions of channels have to be read out in a strong
51 magnetic field (up to 5 T). Compactness and hermeticity of the calorimeters
52 are essential requirements. Plastic scintillator tiles directly read out by silicon
53 pixel photo-detectors operated in Geiger mode are well-suited for this appli-
54 cation; as this kind of photo-detector is small and insensitive to the magnetic
55 field, it can be directly installed onto the scintillator tiles. The coupling be-
56 tween the scintillator and the photo-detector is still under test. A first proposal
57 is to collect the scintillation light via a green wavelength shifting fibre installed
58 in a semicircular groove on the tile itself. Such a set-up is needed when using
59 the green sensitive SiPM. It ensures a light collection which is independent
60 on the incidence position of the detected particle on the scintillator. A sec-
61 ond proposal is to couple the photo-detector directly to the scintillator which
62 would simplify the manufacturing of the calorimeter cells. In this case, the blue
63 sensitivity of MPPC would allow a sufficiently good light collection efficiency.
64 However, the uniformity of the response remains to be proven. Calorimeter
65 prototypes using both methods have been developed and are currently tested
66 in the framework of the International Linear Collider project [5].

67 Positron emission tomography (PET) is a functional imaging technique. A β^+
68 tracer is injected into a living organism and the two 511 keV annihilation pho-

69 tons are detected in coincidence by an array of detectors around the observed
70 biological system. A detector for PET has to provide a good energy resolution
71 of something like 10% at an energy of 511 keV in order to discriminate the
72 signal from the lower energy Compton scattered photons, which constitute the
73 main source of degradation of the image [6]. This is achieved using inorganic
74 scintillators like BGO and LSO. They are better suited for PET application
75 than organic scintillators as they have a higher density and are thus more
76 efficient in detecting 511 keV photons. The traditional detector block for PET
77 tomographs is made of a pixelated array of crystals read out by four photo-
78 multipliers — the signal being reconstructed with a resistive chain weighting
79 technique [7]. Many studies aim at improving the spatial resolution of the
80 system with highly segmented arrays of crystals individually read out by an
81 appropriate photo-detector. Besides, the signal to noise ratio of the image can
82 be enhanced with a more precise localization of the sources, using the time of
83 flight information of the two detected photons (ToF-PET) [8,9]. The SiPM is
84 a natural candidate for this application, due to its small size, high gain and
85 easy read-out circuit. The blue sensitivity introduced with the MPPC is a key
86 feature for PET as it allows a much better energy resolution at 511 keV, com-
87 pared to the green sensitive SiPMs. An application of MPPCs in ToF-PET
88 systems is also under investigation, as the excellent timing response of these
89 new devices makes them competitive to the traditional photomultiplier tubes.
90 In addition, their insensitivity to magnetic field makes them a good candidate
91 for use in combined PET-NMR system.

92 The aim of this study is to investigate whether the light collection efficiency
93 of MPPCs directly coupled to organic and inorganic scintillators (LSO, LSF-
94 7¹) and their timing properties match the benchmark requirements for highly
95 granular calorimetry and positron emission tomography.

96 **1 Description of the test set-up**

97 This study is based on a set of MPPC with different size ($1 \times 1 \text{ mm}^2$ up to
98 $3 \times 3 \text{ mm}^2$) and with different number of pixels (400 up to 1600). Five pieces
99 of each detector type have been available for testing. The suggested operation
100 voltage ranges between 70 V and 78 V. The main properties of the MPPCs
101 tested in this report are shown in Table 1.

102 In the following sections the results of two different studies are described.
103 One is dedicated to the read-out of plastic scintillators using MPPCs (plastic
104 scintillator response study; section 2), the other investigates the properties of
105 directly coupled crystal-MPPC systems (inorganic scintillator response study;

¹ Lutetium Fine Silicate, developed by General Physics Institute, Moscow [10]

size [mm ²]	Number of pixels/mm²	Bias [V]	Gain [10 ⁶]	Dark Rate >0.5 pixels [kHz]	Dark Rate >1.5 pixels [kHz]
1 × 1	400	76	7.4-7.5	220-250	9-10
1 × 1	1600	78	2.6-2.7	50-60	0.05-0.1
3 × 3	400	70	7.4-7.5	3200-3300	320-330

Table 1

Characterization of the MPPC used in this study.

106 section 3). The different test set-ups used for the two studies are described
107 below.

108 For the plastic scintillator response study ¹⁰⁶Ru is used as an electron source
109 delivering minimum ionizing particles (m.i.p.) to be detected via the light
110 they produce in scintillator tiles. Two different 3 × 3 × 0.5 cm³ plastic scin-
111 tillators tiles are used, both manufactured by *Uniplast* enterprise (Vladimir,
112 Russia), which also delivered the tiles of the CALICE hadronic calorimeter
113 prototype [5]. One of the tiles contains a green wavelength shifting fibre (Ku-
114 raray multicladding WLS fibre Y11(200)) of a 0.5 mm radius and t is used
115 to test the traditional fibre-mediated read-out. The second tile has no wave-
116 length shifter installed and is used to investigate the direct read-out of the
117 blue scintillation light produced. Both tiles are wrapped in a Super-radiant
118 VN2000 foil (3M).

119 A second test set-up is operated to study the response of directly coupled
120 crystal-MPPC systems. A ²²Na source is used to provide two coincident
121 511 keV annihilation photons; the analysis is based on the simultaneous de-
122 tection of both photons by a pair of crystals directly coupled to two MPPCs
123 using optical grease. Three different crystal pairs are used for this study. Two
124 pairs of 1 × 1 × 15 mm³ and 3 × 3 × 15 mm³ LSO crystals (Hilger crystals)
125 and one pair of 3 × 3 × 15 mm³ LFS-7 crystals are used in this study. All six
126 crystals are wrapped in a Teflon layer of 2-mm thickness .

127 The relative position and the optical coupling between the scintillators and
128 the MPPC are the most important source of systematic error for both stud-
129 ies. In order to reduce its size different structures are used for coupling the
130 MPPCs to tiles and crystals. For the plastic scintillator response study, the
131 MPPCs are kept fixed to a rigid holder such that for the tile with the wave-
132 length shifter (WLS) the device can be easily positioned in front of the WLS
133 fibre; for the plane tile without a WLS fibre installed the holder is moved
134 to two different well defined points along the edges of the plastic scintilla-
135 tor tile. When studying the inorganic scintillator response the crystal-MPPC

136 systems are fixed and can only move towards or away from the ^{22}Na source.
137 The remaining uncertainty on the energy resolution is estimated by repetitive
138 measurements of the spectra and is found to be 3%, 10% and 15% respectively
139 for the plastic scintillators, the $3 \times 3 \text{ mm}^2$ and the $1 \times 1 \text{ mm}^2$ crystals.

140 The signal of the 1600 pixels MPPC is amplified by a wide-band voltage ampli-
141 fier (Phillips Scientific 6954). The 400 pixels devices do not need amplification.
142 Signal integration is done by a QDC Lecroy 1182, using a gate of 80 ns. For
143 the plastic scintillator response study the QDC is triggered by an additional
144 scintillator which is installed behind the scintillator/MPPC system and read
145 out by a traditional photomultiplier tube. In case of the crystal-MPPC set-up
146 the trigger is provided by a coincidence signal from the two MPPCs formed
147 via standard NIM logic.

148 For timing studies the signals of crystal-MPPC systems are also digitized
149 without any amplification, using a 4-GHz True-Analog Bandwidth oscilloscope
150 (TDS7404B by Tektronix) triggered internally; in acquisition mode it provides
151 a sampling rate of 20 GS/s resulting in a time resolution of 100 ps as two
152 channels are used simultaneously; the digitized signals are stored with an
153 acquisition rate of about ~ 1 Hz for offline analysis.

154 **2 The Read-out of Plastic Organic Scintillators Using MPPCs**

155 *2.1 Comparison Between Direct and Wavelength-shifter Mediated Read-out*

156 Plastic organic scintillators are mainly used to detect charged particles. Hence
157 the most probable value (MPV) for the number of photo-electrons produced
158 in a MPPC when a minimum ionizing particle (m.i.p.) traverses the scintil-
159 lator is chosen as characteristic measure. The typical signal distribution of
160 a scintillator/MPPC system is shown in Fig.1.a. Each peak corresponds to a
161 certain number of pixels firing in the MPPC. The good separation of the peaks
162 indicates the good uniformity of the device. The signal is fitted with a multi-
163 Gaussian function. From this fit the area under each peak is extracted and
164 plotted as a function of the number of pixels fired (Fig. 1.b). The resulting data
165 points follow a Landau distribution smeared by a Poissonian photo-statistics.
166 The maximum of this distribution is the sought-after MPV and estimated
167 with a Gaussian fit to the peak region. Fig. 2 shows the resulting MPV as a
168 function of the over-voltage² for (a) the read-out via WLS fibres and (b) the

² The over-voltage is defined as the difference between the operation bias voltage and the breakdown voltage.

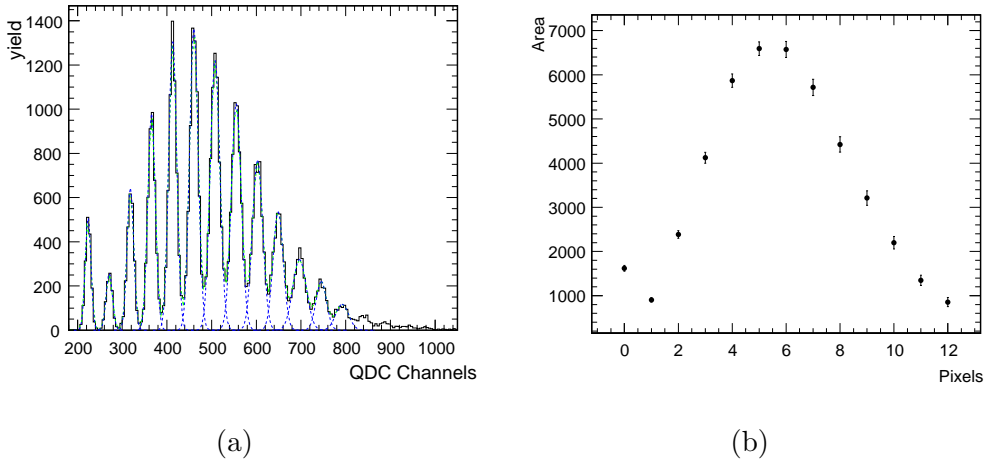


Fig. 1. M.i.p. signal distribution of a scintillator/MPPC system; in this particular example the plastic scintillator tile is directly read out by a 1600 pixels MPPC, operated at 2 V over-voltage. The diagram shows the measured distribution (histogram) together with Gaussian fits (dashed lines) used to determine the area under each individual peak (a) and the area under each peak as a function of the number of pixels fired (b); the maximum of this distribution determines the MPV (see text).

169 direct coupling as detected by the 400 and 1600 pixel MPPC devices³

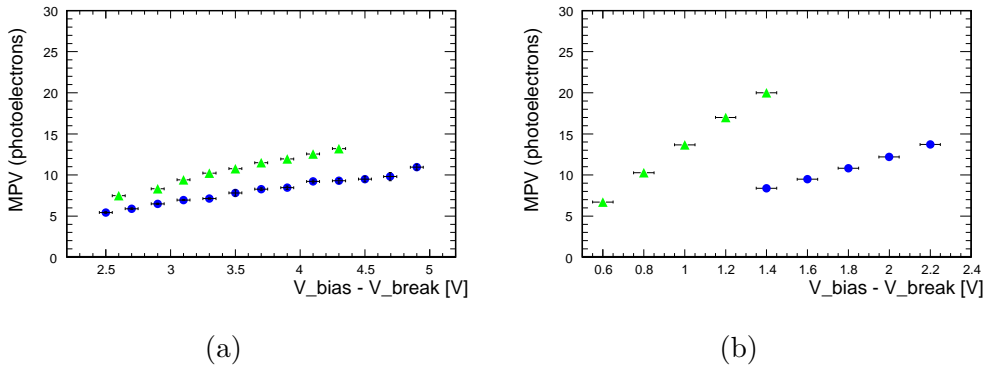


Fig. 2. MPV distribution as a function of the over-voltage; (a) 1600 pixel MPPC and (b) 400 pixel MPPC. The blue dots are the result for a direct scintillator/MPPC coupling, the green triangles those for the wavelength shifter mediated read-out.

170 As a result, the signal size in number of photo-electrons (pixels) is found to be
 171 half as big for the 1600 pixel MPPC compared to the signal size observed with
 172 the 400 pixel device; this is in agreement with expectation when comparing

³ The noise and the allowed precision of the experimental system constrain the minimum number of mean detected photo-electrons to 5. The balance between the amplifier and the input of the QDC limits the maximum number of mean detected photo-electrons approximately to 20. The response of the 400 pixel MPPC could be studied, hence, only for $V_{bias} - V_{break} > 1.4$ V in the direct coupling configuration and for $V_{bias} - V_{break} < 1.4$ V in the wavelength shifter mediated read-out configuration.

173 the photo-detection efficiencies of these devices as quoted in the Hamamatsu
 174 data sheet ⁴. Repeating the measurements for the direct coupling case with the
 175 MPPCs positioned at different locations w.r.t. the tile center (edges, corners)
 176 yields similar results, all compatible within the quoted systematic uncertainty
 177 of 3%.

178 2.2 Implications for Hadronic Calorimetry

179 The most important parameters determining the performance of a calorimeter
 180 are the response and the noise of a single channel. To quantify the response
 181 m.i.p. signals are used as a reference the MPV of the signal produced by a
 182 m.i.p. sets the energy scale for each channel; the signal-to-noise ratio deter-
 183 mines the detection efficiency.

184 The discrimination between noise and physics signals is typically done using
 an amplitude threshold ⁵. The normalized integral of the m.i.p. signal dis-

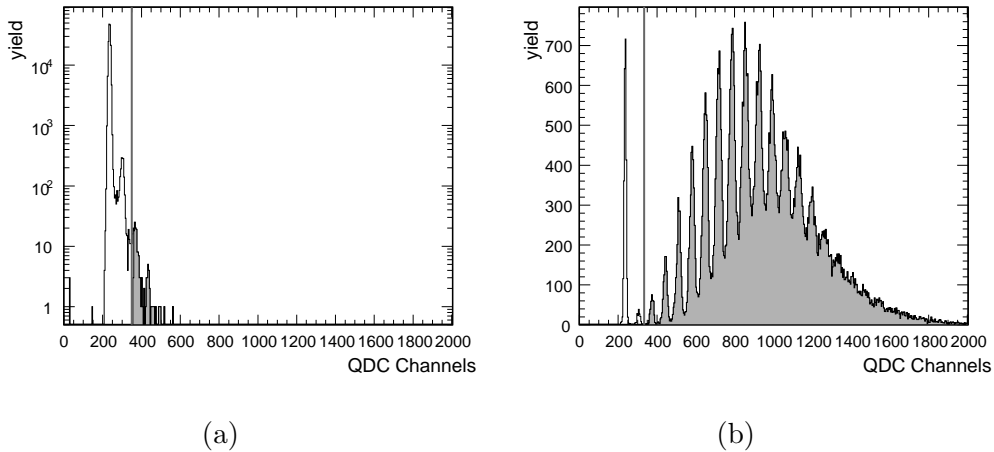


Fig. 3. (a) Noise spectrum of the 400 pixel MPPC; an amplitude threshold (line) is defined requiring that the maximum rate of the remaining noise (shaded area) is 3 kHz; (b) m.i.p. spectrum. The detection efficiency is defined by the shaded area, i.e. the integral of the spectrum above threshold (line).

185 tribution above this threshold determines the m.i.p. detection efficiency. All
 186 signals above threshold constitute a hit in the calorimeter. The procedure is
 187

⁴ The direct comparison between the efficiency quoted in the data sheet and the light yield measured in this experiment is qualitative. While Hamamatsu quotes the response of the MPPC to a monochromatic photon source, the *green* and *blue* light used in this experiment consist of a wide spectrum resulting from the mechanism of scintillation.

⁵ The total charge of the signal is considered as amplitude in this application.

188 depicted in Fig. 3. As the amplitude threshold is determined by the pedestal
 189 noise spectrum (Fig. 3a) lower noise allows for higher detection efficiencies.

190 In practice the amplitude threshold is fixed considering the allowed channel
 191 occupancy. For the ILC calorimeter a relative channel occupancy of 10^{-4} is
 192 required. For a beam crossing interval of 300 ns this translates into a maximum
 193 noise rate of 300 Hz. For the existing 8000 channel hadronic calorimeter 1 m³-
 194 prototype [5] integration time is only 200 ns; the maximum noise rate presently
 195 allowed for test beam studies is 3 kHz resulting in a relative occupancy of
 196 6×10^{-4} .

197 After fixing the amplitude threshold the m.i.p. detection efficiency is calcu-
 198 lated by integrating the m.i.p. spectrum (Fig 3b) above threshold. For the
 199 scintillator/SiPM system used in the ILC calorimeter prototype this proce-
 200 dure yields a 95% detection efficiency; the MPV of a m.i.p. signal observed
 201 for this system is 15 ± 2 photo-electrons.

202 The measured m.i.p. detection efficiencies for the 1600 pixel and the 400 pixel
 MPPCs are shown in Fig. 4 as a function of the over-voltage⁶. Results are

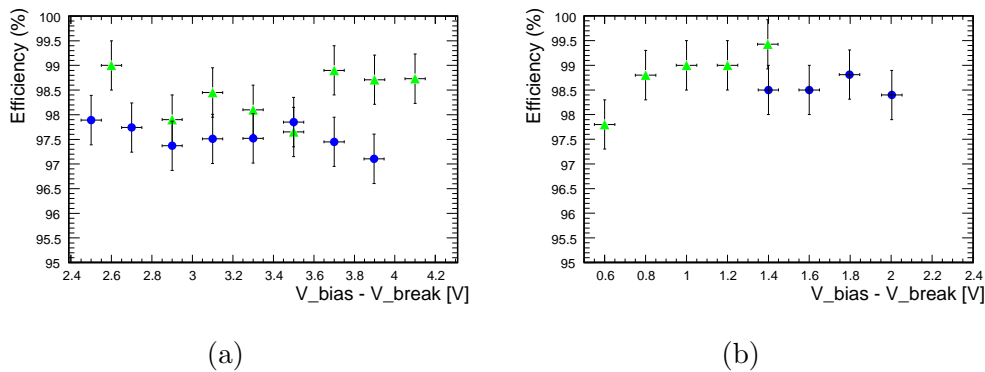


Fig. 4. Signal detection efficiency for a 1600 pixels (a) and a 400 pixels (b) MPPCs. The blue dots are the result for a direct scintillator/MPPC coupling, the green triangles those for the wavelength shifter mediated read-out.

203 shown for both the direct scintillator-MPPC coupling as well as for the wave-
 204 length shifter mediated read-out. Due to a very low dark rate and low cross
 205 talk the MPPCs show very low noise such that with the requirement of 3 kHz
 206 noise rate the amplitude threshold can be set to a value of only 1.5 to 2 pix-
 207 els. Correspondingly a detection efficiency of more than 97% is observed; the
 208 value measured for the wavelength shifter mediated read-out is slightly higher
 209 ($\sim 98\%$). In order to reach these efficiencies the 1600 pixel MPPC must be
 210 operated at an over-voltage of 2.5 V to 3.5 V; in this case the corresponding
 211 MPV of a m.i.p. signal lies between 6 and 7 photo-electrons. In contrast the
 212 400 pixel device must be operated at over-voltages of 0.6 V to 2 V.
 213

⁶ The over-voltage is the biasing voltage relative to the breakdown voltage.

214 For both direct coupling as well as wavelength shifter mediated read-out the
215 1600 pixel MPPC provides a better solution compared to SiPMs as it yields
216 a similar detection efficiency but has a larger dynamic range. For the 400
217 pixel MPPC the detection efficiency is higher than for SiPMs but the reduced
218 number of pixels imposes strict bounds on the dynamic range.

219 It has to be noted that for both MPPC types the dark rate drops rapidly if
220 the amplitude threshold is raised. Thus by using a threshold of 2 to 4 pixels
221 the tighter ILC requirements on the noise can be easily met. In this case it
222 is still possible to operate the MPPCs at an over-voltage such that a m.i.p.
223 detection efficiency of above 95% is obtained. If in the final ILC calorimeter
224 thinner scintillators (e.g. 3 mm instead of 5 mm thickness) are used, the lower
225 light yield may be compensated by a better coupling or a larger sensitive area
226 of the photo-detector (e.g. $3 \times 3 \text{ mm}^2$). Further studies are needed in order to
227 prove the applicability of MPPCs under such conditions.

228 **3 Direct Read-out of LSO and LFS Crystals Using MPPCs**

229 *3.1 Energy resolution of a crystal-MPPC system*

230 The energy spectrum of 511 keV photons measured with one detector is pre-
231 sented in Fig. 5. The photo-electric peak is clearly separated from the energy
232 continuum of Compton-scattered photons. The energy resolution of the de-
233 tector is extracted using a Gaussian fit to the peak region. The ratio of the
234 FWHM over the mean of the fit is quoted as an estimate for the energy res-
235 olution. An energy resolution of $10.0\% \pm 0.3\%(stat) \pm 1\%(sys)$ is obtained
236 for the $3 \times 3 \times 15 \text{ mm}^3$ system (Fig. 5a), while $14\% \pm 0.4\%(stat) \pm 2\%(sys)$
237 is measured with the $1 \times 1 \times 15 \text{ mm}^3$ system (Fig. 5b). The lower statistics
238 of Fig. 5b with respect to Fig. 5a is due to the reduced acceptance of the
239 $1 \times 1 \times 15 \text{ mm}^3$ system. The rather large systematic uncertainties on the re-
240 sult for the $1 \times 1 \times 15 \text{ mm}^3$ system measurements are due to a still imperfect
241 setup of the test system. Improvements are possible especially concerning the
242 technical reproducibility and the crystal-MPPC coupling. The finite number
243 of pixels of the MPPC causes its response to be non-linear at high photon
244 fluxes.

245 The effect of the non-linearity of the MPPC on the energy scale is investigated
246 measuring the response of the system to photon radiation from ^{137}Cs (662
247 keV), ^{122}Ba (80 keV, 320 keV) as well as ^{22}Na (511 keV). Fig. 6 shows a linear
248 response in the region of interest, up to 622 keV.

249 The signal corresponding to the photo-electric interaction of a 511 keV photon

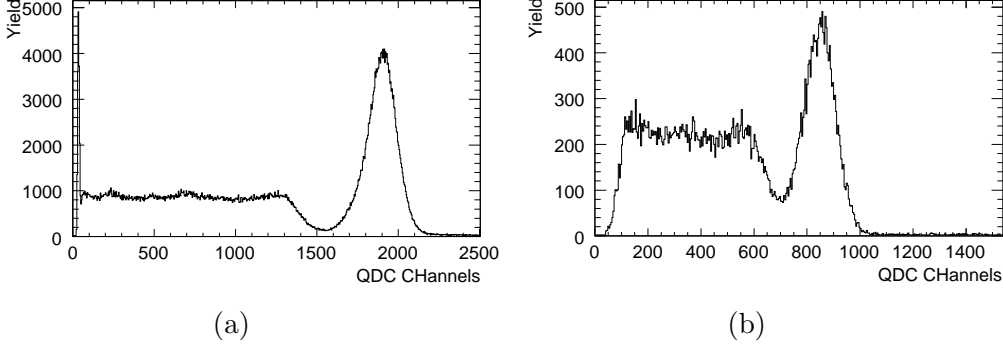


Fig. 5. Energy response to 511 keV photons of (left figure) a $3 \times 3 \times 15 \text{ mm}^3$ LSO crystal coupled to a $3 \times 3 \text{ mm}^2$ MPPC (3600 pixels), and (right figure) of $1 \times 1 \times 15 \text{ mm}^3$ LSO crystal coupled to a $1 \times 1 \text{ mm}^2$ MPPC (400 pixels). The 511 keV photons are provided by a ^{22}Na source

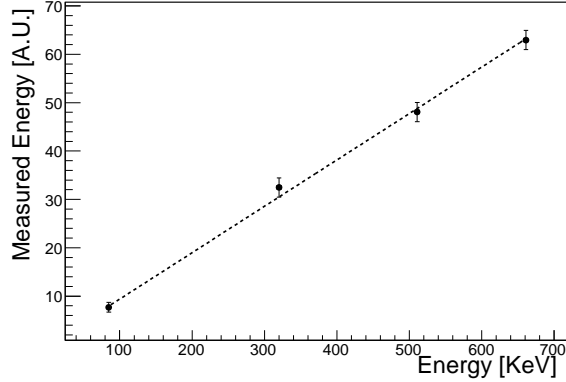


Fig. 6. Linearity of the energy response of a $3 \times 3 \times 15 \text{ mm}^3$ LSO crystal coupled to a $3 \times 3 \text{ mm}^2$ MPPC (3600 pixels).

250 in the LSO crystal is shown in Fig. 7. Note that although the overall number
 251 of photons is large the photon flux from the crystal is quite small. The photons
 252 are emitted over a wide time window of more than 40 ns. As the recovery time
 253 of the MPPC is only about 4 ns the pixels recover fast compared to the dura-
 254 tion of light emission, and the saturation mechanism is strongly suppressed.
 255 The amplitude of the signal, rescaled to the single photoelectron size, gives
 256 an indicative order of magnitude of the time distribution of the detected pho-
 257 tons⁷. The instantaneous amplitude never exceeds 500 photo-electrons. The
 258 probability that two or more photons are detected in the same pixel is hence
 259 minimal in this setup, as a maximum flux of 500 photo-electrons is distributed
 260 on 3600 pixels and on a total active area of $3 \times 3 \text{ mm}^2$.

261 The measurements were repeated for the $3 \times 3 \times 15 \text{ mm}^3$ LFS crystal. They
 262 result in an energy resolution of 11% (Fig. 8), which is comparable to the mea-
 263 surement using the same sized LSO crystal, within the systematic uncertainty.

⁷ The integral is directly proportional to the total number of photo-electrons.

265 *3.2 Time Resolution*

266 The time resolution of the system is determined by measuring the time dif-
 267 ference between the two signals of two back to back scattered photons. As an
 268 estimate of the time resolution, the FWHM of the time difference distribution
 269 is taken. For the measurement of the signal timing, a fixed amplitude thresh-
 270 old is used in this study instead of the constant fraction discriminator method
 271 traditionally used in Tof-PET system. This is justified due to the fast response
 272 of the LSO crystals together with the fast rise time of the large photo-electron
 273 signal of the MPPCs, and significantly simplifies the read-out electronics. It
 274 requires the calibration of each detector cell to the same light yield which is
 275 easily achieved tuning the bias voltage of the MPPCs.

276 The two signals from the detector elements are directly sent to the inputs of the
 277 oscilloscope, where they are discriminated if above a tuneable threshold. This
 278 threshold is kept at approximately 4 mV (or ~ 13 -15 pixels). The minimum
 279 allowed threshold is constrained by the electronic noise level (2.0 ± 0.5 mV
 280 corresponding to 10 ± 1 photo-electrons). A coincidence is formed after the
 281 discrimination and used as trigger to store the full signal waveform starting
 282 considerably before the trigger time. The offline analysis is, hence, independent
 283 from the coincidence threshold.

284 The timing measurement is mainly influenced by the selection of the signals
 285 and the timing threshold as it was previously shown in [11]. Fig. 9 illustrates
 286 the improvement in time resolution obtained when applying an energy cut of
 287 $\pm 1\sigma$ around the photo-electric peak value. When selecting only events with
 288 energies near the photo-electric peak a sharp time difference distribution is

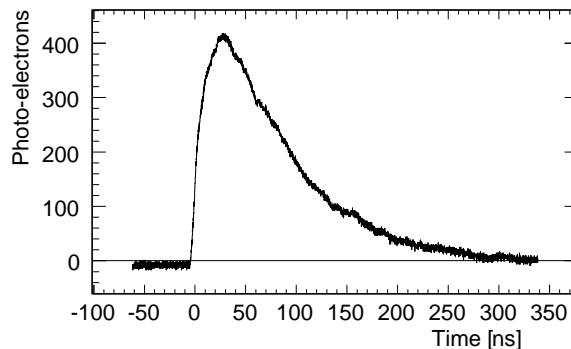


Fig. 7. Photo-electric signal of a 511 keV photon detected by a $3 \times 3 \times 15$ mm³ LSO crystal coupled with a 3×3 mm² MPPC with 3600 pixels. The signal amplitude is shown in unit of a single photo-electron signal.

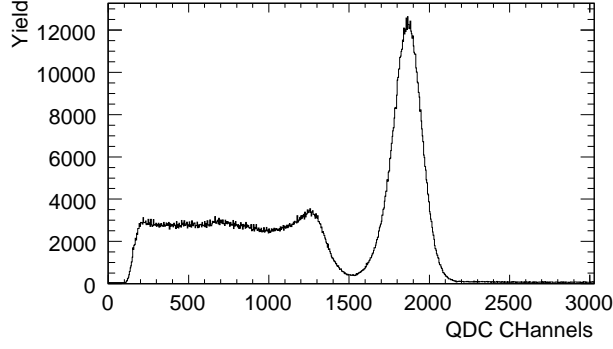


Fig. 8. Energy response to 511 keV photons of a $3 \times 3 \times 15$ mm³ LFS crystal coupled to a 3×3 mm² MPPC (3600 pixels). The 511 keV photons are provided by a ²²Na source

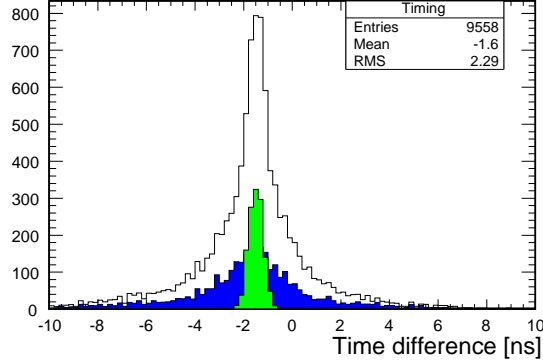


Fig. 9. Time resolution of a system of two $3 \times 3 \times 15$ mm³ LSO crystals directly read out by two MPPCs of the same size. The total sample, without cuts, is shown as a black line. The sharp signal peak (green) corresponds to the events with energies near the 511 KeV photoelectric peak in both crystals. The blue background corresponds to the events in which one of the two photons loses energy through the Compton effect.

289 observed (green). Its FWHM is measured to be 647 ± 3 ps, estimated with a
 290 gaussian fit in the interval $\pm 2\sigma$ around the mean value. The events in which
 291 one or both photons undergo Compton scattering are the main background of
 292 the measurement. The timing spread of these events is widely distributed and
 293 ruins the time resolution of the system (blue). This effect can be directly ex-
 294 trapolated from the signal shapes observed on the oscilloscope. Photons which
 295 undergo Compton scattering are observed as signals of smaller amplitude and
 296 slope if compared to signals from photons depositing their full energy inside
 297 the crystals.

298 The influence of the chosen threshold on the time resolution is shown in Fig. 10.
 299 The time resolution degrades fast with increasing coincidence threshold, as
 300 the measurement becomes more sensitive to the variation of the rise time of

301 the signals. The improvement of the observed time resolution when selecting
 302 events from the photo-electric peak is almost a factor of 2.
 303 In order to fully benefit from the fast intrinsic time resolution of the MPPC the
 304 coincidence threshold should in principle be lowered to below the amplitude
 305 corresponding to a single photoelectron. However, this region is outside the
 306 dynamic range of the current instrumentation and can be analysed only after
 307 improving the present set-up.

308 3.3 Implications for the design of a PET system

309 As the traditional photo-detector commonly used in PET is the photomultiplier
 310 a comparison between the obtained results and the typical performances
 311 of a PET detector block explicates the good perspectives of the use of MPPCs
 312 in this field. The measured energy resolution allows an efficient separation
 313 between the photoelectric peak and the Compton scattered events. In similar
 314 experiments [12,13], it has been shown that the traditional SiPM (from CPTA
 315 and MEPHI) coupled to a $3 \times 3 \times 15 \text{ mm}^3$ crystal provides a resolution of about
 316 25-35% due to the poor photo-detection efficiency in the blue spectral region.
 317 LSO crystals show a $\sim 10\%$ energy resolution for 511 keV photons when read
 318 out by a traditional photomultiplier tube [8] (mainly originating from the
 319 LSO intrinsic energy resolution of about 9% [14]). The results obtained indi-
 320 cate that the MPPC provides an energy resolution for PET application which
 321 is competitive with that of PMT with the advantage of an easy direct coupling
 322 to a small crystal. Using MPPC for a PET detector would thus allow to reduce
 323 the single crystal pixel size down to 1 mm^2 improving the spatial resolution
 324 of the scanner. Improvements in the reconstruction of the depth of interaction
 325 using multi-layer imaging modules are also currently under investigation [15].

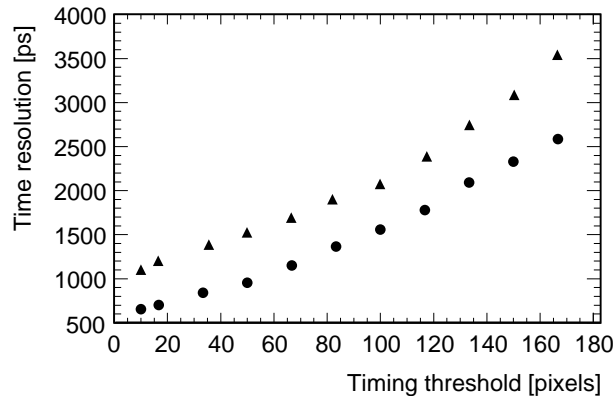


Fig. 10. Time resolution as a function using fixed amplitude threshold for a system of two $3 \times 3 \times 15 \text{ mm}^3$ LSO crystals coupled to $3 \times 3 \text{ mm}^2$ MPPC 3600 pixels using fixed amplitude threshold. Results obtained with (points) and without (triangles) energy cut are shown (see text).

326 The obtained time resolution is compatible with the typical value quoted in
327 similar studies — 475 ps in [9] — suggesting a possible application of MPPCs
328 also to ToF-PET.

329 4 Conclusions

330 This study shows that the Multi Pixel Photon Counter represents an effective
331 technological improvement of the silicon pixel photo-detectors operated in
332 Geiger mode. The new key-feature of this photo-detector is the blue sensitivity,
333 which allows the direct read-out of scintillators, both organic and inorganic,
334 with high efficiency.

335 The measured light yield corresponding to a m.i.p. particle detected by a plas-
336 tic scintillator tile with size $3 \times 3 \times 0.5 \text{ cm}^2$, directly read out by a MPPC
337 on the edge, is 10-15 photoelectrons. The low dark rate of this device allows
338 discriminating the m.i.p. signal from the noise with a threshold at 1.5-3 pho-
339 toelectrons, yielding high m.i.p. signal collection efficiency. The 1600 pixels
340 MPPC matches most of the requested parameters for a possible application in
341 hadronic calorimetry, although uniformity and stability of a large sample need
342 to be proved. The issue of the uniformity of the response over a scintillator
343 tile with direct read-out still has to be investigated.

344 The energy resolution of a $3 \times 3 \times 15 \text{ mm}^3$ LSO crystal, directly read out by
345 a MPPC with an active area of the same size, reaches 10% FWHM and a
346 timing resolution of 650 ps. Slightly worse results - $\sim 14\%$ energy resolution
347 - are obtained with the $1 \times 1 \text{ mm}^2$ crystals and photo-detectors, mainly due
348 to systematic effects in the alignment of the setup. More systematic studies
349 of the $1 \times 1 \text{ mm}^2$ MPPC as well as of the energy and timing behaviour of
350 the LFS crystals will follow. This MPPC/crystal detector system fulfils the
351 strongest requirement for a positron emission tomography scanner. In addi-
352 tion, the MPPC would allow a significant simplification of the technological
353 design and of the read-out electronics.

354 Acknowledgments

355 This work is supported by the Helmholtz-Nachwuchsgruppen grant VH-NG-
356 206 and the BMBF, grant no. 05HS6VH1. We thank V. Korbelt, V. Saveliev
357 and F. Sefkow for their useful suggestions and comments. We thank Hama-
358 matsu, which kindly provided us the tested samples of MPPC. We thank V.
359 Koslov and A. Terkulov from LPI for providing the LFS. We thank also Peter
360 Smirnov for his professional technical support.

361 **References**

- 362 [1] V.Saveliev, V.Golovin, Silicon avalanche photodiodes on the base of metal-
363 resistor-semiconductor (mrs) structure, Nucl. Instr. Meth. A442 (2003) 223.
- 364 [2] P.Buzhan, et al., Silicon photomultiplier and its possible applications, Nucl.
365 Instr. Meth. A504 (2003) 48.
- 366 [3] Z.Sadygov, et al., Super-sensitive avalanche silicon photodiode with surface
367 transfer of charge carriers, Nucl. Instr. Meth. A504 (2003) 301.
- 368 [4] Hamamatsu, Multi-pixel photon counter, datasheet, Tech. rep. (2006).
369 URL www.hamamatsu.com
- 370 [5] T.Behnke, C. Damerell, J.Jahros, A. Miyamoto, International Linear Collider.
371 Reference design report. Detectors, 2007.
- 372 [6] J.L.Humm, A.Roszenfeld, A. D. Guerra, From pet detectors to pet scanners,
373 Eur. Jour. Nucl. Med. 30 (11) (2003) 1574.
- 374 [7] P.Valk, D. Bailey, D. Townsend, M. Maisey, Positron Emission Tomography,
375 2003.
- 376 [8] W.W.Moses, Recent advances and future advances in time-of-flight pet, Nucl.
377 Instr. Meth. A30 (2007) 1574.
- 378 [9] W.W.Moses, Prospects for time-of-flight pet using lso scintillator, IEEE Trans.
379 Nuc. Sci. (NS-46) (1999) 474.
- 380 [10] A.I.Zagumennyi, Yu.D.Zavartsev, S.A.Kutovoi., Us patent 7132060.
- 381 [11] N.D'Ascenzo, E.Eggeman, E.Garutti, A. Tadday, Application of the micro pixel
382 photon counter to hadron calorimetry and pet, Il Nuovo Cimento 30C (2007)
383 463.
- 384 [12] D. Herbert, N. D'Ascenzo, N. Belcari, A. Del Guerra, F. Morsani, V. Saveliev,
385 Study of sipm as a potential photo detector for scintillator readout, Nucl. Instr.
386 Meth. A567 (2006) 356.
- 387 [13] A. Otte, J. Barral, B. Dolgoshein, J. Hose, S. Klemin, E. Lorenz, R. Mirzoyan,
388 al., A test of silicon photomultipliers as readout for pet, Nucl. Instr. Meth. A545
389 (2005) 705.
- 390 [14] M.Balcerzyk, et al., Yso, lso, gso and lgso. a study of energy resolution and
391 nonproportionality, IEEE Trans. Nuc. Sci. 47 (2000) 1319.
- 392 [15] D. Herbert, S. Moehrs, N. D'Ascenzo, N. Belcari, A. Del Guerra, F. Morsani,
393 V. Saveliev, The silicon photomultiplier for application to high resolution
394 positron emission tomography, Nucl. Instr. Meth. A573 (2007) 84.